Development 134, 1873-1885 (2007) doi:10.1242/dev.001495

pygopus 2 has a crucial, Wnt pathway-independent function in lens induction

Ni Song[1,2,3,4], Kristopher R. Schwab[5], Larry T. Patterson[6], Terry Yamaguchi[7], Xinhua Lin[2,4], Steven S. Potter[2,4] and Richard A. Lang[1,2,3,4,*]

Drosophila Pygopus was originally identified as a core component of the canonical Wnt signaling pathway and a transcriptional coactivator. Here we have investigated the microophthalmia that arises in mice with a germline null mutation of pygopus 2. We show that this phenotype is a consequence of defective lens development at inductive stages. Using a series of regionally limited Cre recombinase transgenes for conditional deletion of *Pygo2^{flox}*, we show that Pygo2 activity in pre-placodal presumptive lens ectoderm, placodal ectoderm and ocular mesenchyme all contribute to lens development. In each case, Pygo2 is required for normal expression levels of the crucial transcription factor Pax6. Finally, we provide multiple lines of evidence that although Pygo2 can function in the Wnt pathway, its activity in lens development is Wnt pathway-independent.

KEY WORDS: Pax6, pygopus 2, Wnt, Lens induction, Mesenchyme, Neural crest, Mouse

INTRODUCTION

The vertebrate lens is a classical model system in which to study developmental mechanisms. Since the experiments of Spemann (Spemann, 1901) we have understood that signals from the optic vesicle are required for lens development. The lens originates from embryonic head surface ectoderm. In the mouse, prior to any morphological sign of lens development, presumptive lens ectoderm (PLE) and optic vesicle are separated by a few cell layers of neural crest-derived mesenchyme. In the chick, ocular mesenchyme (OM) flanks but does not separate the epithelia of the forming eye and defines the lens through an inhibitory mechanism (Sullivan et al., 2004). In the mouse, epithelia of the optic vesicle and PLE make close contact just before formation of the lens placode, a thickened region of epithelium that is the first morphological sign of lens development. After the lens placode has formed, it invaginates in coordination with the optic cup and forms the lens pit. The lens pit closes spherically to form the lens vesicle and separates from the surface ectoderm. The transparent and refractile fiber cells of the mature lens begin their differentiation from the proximal wall of the lens vesicle.

Molecular genetic analysis has established model pathways for the regulation of lens induction (Lang, 2004). Currently, the apex of these pathways is occupied by the paired and homeodomain transcription factor Pax6. *Pax6* is necessary, and in *Xenopus* embryo assays also sufficient, for lens induction (Chow et al., 1999; Ashery-Padan et al., 2000). In the mouse, there are two phases of *Pax6* expression in the PLE. The early, so-called pre-placodal phase, corresponds to the head surface ectoderm of the E8.5 mouse embryo (Grindley et al., 1995). Later, *Pax6* is upregulated in a smaller, placodal region domain (defined as *Pax6^{placode}*). Assessment of *Pax6* transcription in the *Pax6^{Sey}*-null mutant (Hill et al., 1991) has shown that the placodal phase of *Pax6* expression is dependent on the pre-placodal Pax6 (Grindley et al., 1995; Lang, 2004). The placodal phase of *Pax6* expression is also dependent on Fgf receptor activity (Faber et al., 2001; Gotoh et al., 2004) and Bmp7 signaling (Wawersik et al., 1999), as well as Meis family transcription factors (Zhang et al., 2002). It has been shown that Bmp4 signaling regulates *Sox2* expression in the presumptive lens (Furuta and Hogan, 1998) and that Sox2 functions in cooperation with Pax6 to regulate some aspects of lens development (Kamachi et al., 2001).

The canonical Wnt pathway has a crucial role in development and disease (Nusse, 2005). A family of lipid-modified Wnt ligands (Willert et al., 2003) can activate a receptor complex comprising a multi-transmembrane-pass Frizzled family member and a co-receptor of the Arrow/Lrp5/Lrp6 class (He et al., 2004). Activation of this complex initiates signal transduction culminating in stabilization of β-catenin, its association with Lef/Tcf family transcription factors (Eastman and Grosschedl, 1999) and target gene regulation. The Wnt pathway is suggested to be inhibitory to early lens development and to restrict the region of surface ectoderm that can form lens (Smith et al., 2005). Defects in the *Lrp6*-null mouse also suggest that Wnt signaling is required for lens epithelial integrity and differentiation (Stump et al., 2003).

Pygopus was identified as a core component of the Wingless(Wg)/Wnt signaling pathway in *Drosophila* (Belenkaya et al., 2002; Kramps et al., 2002; Parker et al., 2002; Thompson et al., 2002). Pygopus exists in a complex with Armadillo/β-catenin, Legless/Bcl9, Pan/Tcf and parafibromin (CDC73)/Hyrax and has an essential co-activator function (Mosimann et al., 2006). Pygopus incorporates N-terminal homology and plant homology domains (NHD, PHD) crucial for activity (Thompson, 2004; Tolwinski and Wieschaus, 2004; Townsley et al., 2004; Hoffmans et al., 2005; Stadeli and Basler, 2005). In the fly, *pygopus* loss-of-function results in many defects that are very similar to *wg* loss-of-function (Belenkaya et al., 2002; Parker et al., 2002). Morpholino inhibition studies in *Xenopus* have shown that the *Pygo2* orthologs *Pygo2α* and *Pygo2β* regulate Wnt pathway responses (Belenkaya et al., 2002; Lake and Kao, 2003) as well as expression of eye markers

Divisions of [1]Pediatric Ophthalmology and [2]Developmental Biology, Children's Hospital Research Foundation, Cincinnati, OH45229, USA. [3]Department of Ophthalmology and [4]Graduate Program of Molecular and Developmental Biology, College of Medicine, University of Cincinnati, Cincinnati, OH45229, USA. [5]Department of Pathology, University of Michigan, 109 Zina Pitcher Drive, Ann Arbor, MI48109, USA. [6]Division of Nephrology, Children's Hospital Research Foundation, Cincinnati, OH45229, USA. [7]Cancer and Developmental Biology Laboratory, Cell Signaling in Vertebrate Development Section, National Cancer Institute, Frederick, MD 21701-1201, USA.

*Author for correspondence (e-mail: Richard.Lang@cchmc.org)

Accepted 27 February 2007

such as *Pax6*, *Rx-1* and *BF-1* (Lake and Kao, 2003). Some analyses have suggested that *pygopus* has functions outside the Wnt pathway (Belenkaya et al., 2002; Parker et al., 2002).

There are two *pygopus* homologs in the mouse: pygopus 1 (*Pygo1*) and pygopus 2 (*Pygo2*) (Li et al., 2004). To date, their in vivo functions have not been investigated. Here, we examined the consequences of germline and somatic mutation of *Pygo1* and *Pygo2*. Germline *Pygo2* mutation results in microophthalmia that is a consequence of a defect in lens induction. Using a series of Cre recombinase drivers and the conditional allele for *Pygo2*, we show that Pygo2 in the OM and PLE cooperate to promote lens development. Finally, we show that although Pygo2 can regulate normal activity of the Wnt pathway in the OM, loss of mesenchymal Wnt pathway activity has no consequence for lens development. Combined, these data indicate that Pygo2 has a crucial, Wnt pathway-independent role in lens induction.

MATERIALS AND METHODS

Animal use

Mice were housed in a pathogen-free vivarium according to institutional policies. Genetically modified mice used were: *BatlacZ* (Nakaya et al., 2005), *Pax6*^{Sey} (Hill et al., 1991), *Le-cre* (Ashery-Padan et al., 2000), *Wnt1-cre* (Danielian et al., 1998), *Z/EG* (Novak et al., 2000), *Ap2α-cre* (Macatee et al., 2003) *β-catenin* (*Ctnnb1*) conditional loss-of-function (*Catnb*^{tm2Kem}) (Brault et al., 2001) and *β-catenin* conditional gain-of-function (*Catnb*$^{lox(ex3)}$) (Harada et al., 1999).

Gene targeting

The *Pygo1*^{flox} and *Pygo2*^{flox} alleles were generated using standard techniques (Joyner, 1995; Bell et al., 2003) with the constructs shown (Fig. 1). Genomic segments required for the constructs were generated by PCR from RI ES cell DNA. For *Pygo1*, primers (5′ to 3′) used for PCR were: 5′ forward, GTGAAGGAGAGATGGATAAGTATG; 5′ reverse, TAGACCCTAACCACCTACAAG; exon forward, GGTTAGGGTCTATGTGCTGG; exon reverse, TCACCAAATCTCTGTTCTACAC; 3′ forward, TGTGTAGAACAGAGATTTGGTG; and 3′ reverse, CAGTGAAGAAAGAGGGTCAG.

For *Pygo2*, primers (5′ to 3′) used for PCR were: GCCTGGGTTGCTTGTCTTCTG and CCACCTTACTTGTGTGTGAGGATACATAC; CCAAGTCCCAGCATCTCTTAC and CCAGTCATACCAGCAACAAG; and exon sequences TGGGTGCTGGGAACAGAAC and CAACAACAACAGAAGACAAGC.

Targeting constructs were electroporated into ES cells, selected colonies picked and expanded and ES cell lines screened for correct gene targeting as follows. For the *Pygo2* gene, a 1634 bp single-copy flanking probe was prepared by PCR (using primers 5′-CTTCAACATCCACTTCTTCAGTCTTTC-3′ and 5′-TGACACCCACACAGCCATCTTC-3′) and used to probe a Southern blot of *Bst*EII-digested ES DNA. An 8 kb band indicated incorrect targeting, whereas a 9.7 kb band indicated correct targeting. In addition, the Southern blot was hybridized with a neomycin resistance gene (*Neo*) probe to insure that there was a single insertion of the targeting construct. We also performed PCR with the primers 5′-GCTCCTTTCCCTTCCTTTTTGAG-3′ and 5′-ACCAGCAACAAGAAGAATCCAGGC-3′ to insure that the enclosed *loxP* sequence was not deleted by targeting recombination. The end of the insertion that was not confirmed by Southern blotting was checked by PCR using 5′-CTCTGATCCTCACACTTTAG-3′ and 5′-GCATACATTATACGAAGTTATGG-3′, which gave the 5769 bp product indicative of correct targeting. Screening of *Pygo1* ES cell lines was performed by PCR only, first amplifying ES DNA with one external flanking and one internal flanking primer (5′-GCGGATAGGCAGCAGAGAACG and 5′-GGTCGGAGTTTGGATTCGGTG-3′, respectively). In addition, we performed PCR with 5′-AAGCGTGCCTCATCTCCATCCCTAAG-3′ and 5′-GCCCTCCCCGACGTTTATATTG-3′ to confirm retention of the enclosed *loxP* sequence following targeting.

Germline *Pygo1- and Pygo2*-null alleles were generated by mating heterozygous floxed mice with *CMV-cre* mice (Schwenk et al., 1995). Primers used for genotyping PCR were:

Pygo2-null, forward (F) 5′-CCTGGATTCTTGTTGCTGGTATG-3′ and reverse (R) 5′-AAGGTATTTGGTGCTCCGAGGG-3′;
Pygo2 WT or floxed, F 5′-TGTCTTGATGACAGCGTTTAGCC-3′ and R 5′-AGATTCAGTAAGCTGAGCCTGGTG-3′;
Pygo1-null, F 5′-AGTTTGAAATAGCGACGAGTTTGAG-3′ and R 5′-CACTTCTGCCCCTCTCTTTGC-3′; and
Pygo1 WT or floxed, F 5′-AAGCGTGCCTCATCTCCATCCCTAAG-3′ and R 5′-GCCCTCCCCGACGTTTATATTG-3′.

Tissue labeling

Immunofluorescence (IF) labeling was performed as previously described (Smith et al., 2005). Primary antibodies were: anti-Pax6 (1:1000, Covance PRB-278P), anti-β-catenin C-terminus (1:2500, Sigma C2206), anti-GFP-Alexa Fluor 594 (1:1000, Molecular Probes A-21311), anti-β-crystallin (1:5000, generated in our laboratory), anti-Ap2α (1:500, Iowa Hybridoma Bank 3b5) and anti-Sox2 (1:1000, Chemicon AB5603). Human PYGO2 antiserum (1:5000) (Popadiuk et al., 2006) was pre-adsorbed with *Pygo2*$^{-/-}$ mouse embryo powder (4 mg powder per 1 μl antisera) at 4°C for 4 hours. Alexa Fluor secondary antibodies were used at 1:1000 to 1:8000 (A-11072, A-11020, A-11070, A-11017, A-12381, Molecular Probes). For visualization of nuclei we used the Hoechst 33342 counterstain (Sigma B-2261). Pygo2 IF required an antigen retrieval method as previously described (Robinson and Vandre, 2001). Embryos were stained for β-galactosidase (β-gal) activity as described previously (Smith et al., 2005).

Reverse transcription-polymerase chain reaction (RT-PCR)

RNA from isolated tissues was purified using the RNAqueous-4PCR Kit (Ambion 1914) and RT-PCR performed using the OneStep RT-PCR Kit (Qiagen 210212). Semi-nested primers were used for a second round of PCR amplification. Primers used were: *Pygo2*, F 5′-CCCTGAAAAGAAGCGAAGAA-3′ and R 5′-AACTTCCTCCAGCCCATTTT-3′; *Pygo2*, second round R 5′-AACTTCCTCCAGCCCATTTT-3′. PCR products were verified by restriction enzyme digestion.

Quantification of lens size

Equatorial lens diameter was measured on images of E12.5 cryosections and expressed as a ratio to optic cup diameter. The data were represented on a box plot generated using SPSS software. Statistical significance was determined by one-way ANOVA analysis.

Quantification of the Pax6:Ap2α IF signal ratio

To measure the level of Pax6 IF signal in lens placode, we compared the Pax6 signal intensity with that of Ap2α, an internal, unchanging control. Captured images were exported first to Photoshop (Adobe), where control and mutant images from a single labeling experiment were combined. This multi-panel figure was then exported to ImageJ, line intervals drawn through the placodal nuclei and red and green channel intensity histograms obtained as shown in Fig. 4M,N and Fig. 5M,N. To normalize the Pax6 signal to that of Ap2α, the intensity profiles for the red (Ap2α) and green (Pax6) channels for control samples were adjusted so as to be coincident. Since this procedure was performed on an image file that contained both control and mutants, normalization for each was identical. Given that intensity profiles for control samples were arbitrarily coincident, the Pax6:Ap2α intensity ratio was close to 1. For all samples, average intensity values from the placodal line intervals for the red and green channels were obtained and expressed as a ratio representing a single sample. Ratios from multiple control and mutant samples were then combined to produce the box plot shown in Fig. 5L.

RESULTS

Generation of *Pygo1* and *Pygo2* mutant mice

To investigate the role of pygopus genes in mouse, we generated Cre recombinase conditional alleles (*Pygo1*^{flox}, *Pygo2*^{flox}). Germline null alleles (*Pygo1*$^{-}$, *Pygo2*$^{-}$) were generated by crossing *Pygo1*^{flox} and *Pygo2*^{flox} with the *CMV-cre* transgenic line (Schwenk et al., 1995). PCR genotyping on litters generated from crosses of heterozygotes gave the expected amplification products (Fig. 1B,D). RT-PCR on

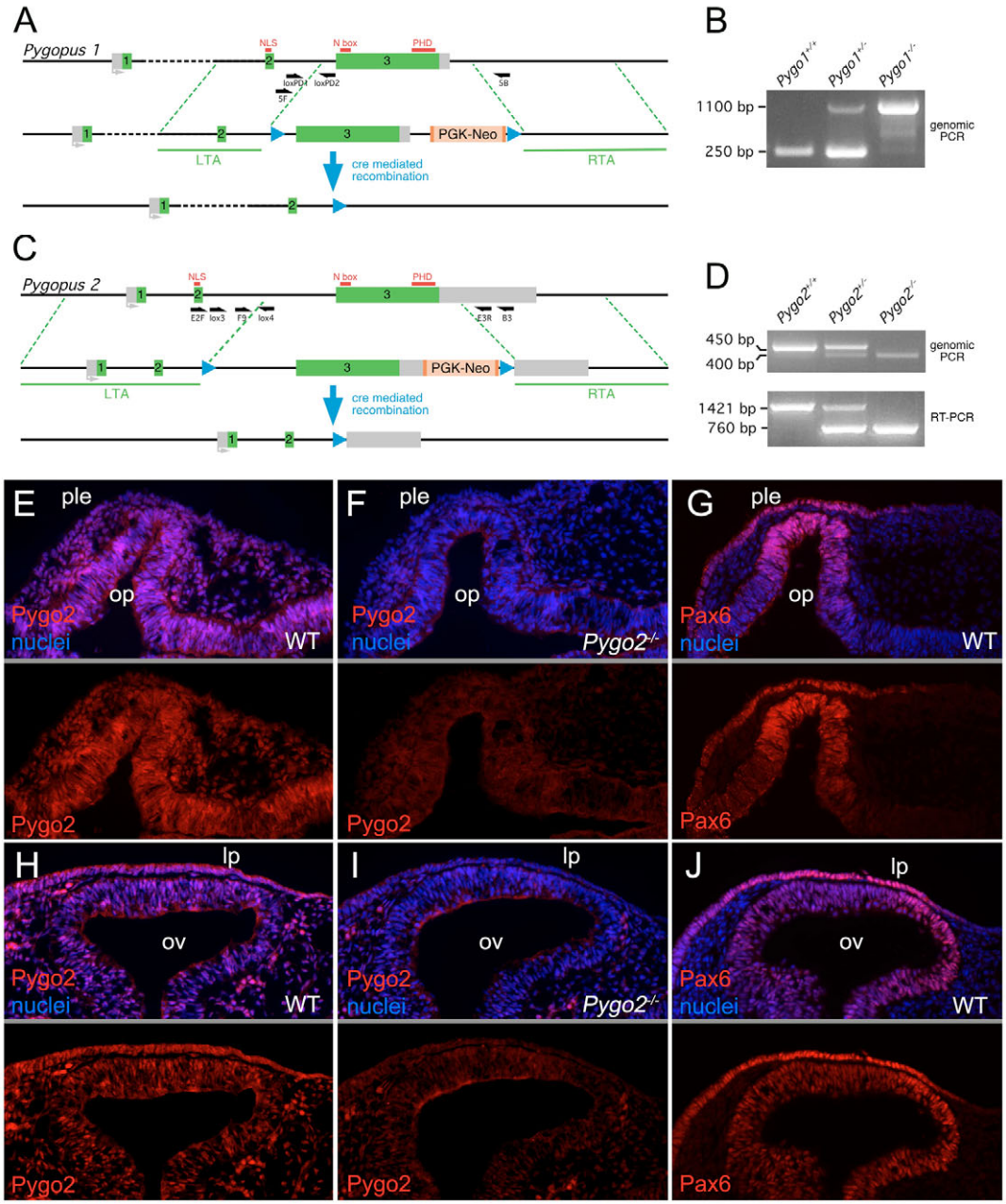

Fig. 1. *Pygo1* and *Pygo2* mutant alleles and expression of Pygo2 in the early mouse eye. (**A**,**C**) Gene targeting for *Pygo1* and *Pygo2* alleles. Green and gray boxes represent coding and non-coding exons, respectively. Light orange box indicates positive selection marker *Pgk-Neo*. Dark orange bars are *frt* sites. Blue arrowheads denote *loxP* sites. The left and right targeting arms (LTA and RTA), N box, PHD domain and nuclear localization signal (NLS) are indicated. Exons are numbered. Black arrows indicate the location of amplification primers used in B,D. (**B**,**D**) PCR amplification of genomic DNA or cDNA (the lower panel in D) for *Pygo1* (B) or *Pygo2* (D) allelic series. (**E-J**) Immunofluorescence for Pygo2 (E,F,H,I) or Pax6 (G,J) in eye region cryosections from the embryonic stages and genotypes indicated. A gray line between panels indicates that different channels of the same image are displayed. ple, presumptive lens ectoderm; op, optic pit; lp, lens placode; ov, optic vesicle.

RNA from embryonic day (E) 9.5 embryos showed that the *Pygo2*$^{-/-}$ mutant had a transcript that was shorter by the anticipated amount (Fig. 1D). *Pygo1* germline null homozygotes were viable and had no obvious phenotype. By contrast, most *Pygo2* homozygotes died neonatally with the occasional mouse surviving to adulthood. *Pygo2* homozygotes were smaller than wild-type (WT) littermates in late gestation and are known to have a mild kidney development defect (Schwab et al., 2007). Currently, the cause of neonatal lethality is unknown. Interestingly, *Pygo2* homozygotes showed a severe microophthalmia that is the focus of this study.

Developmental expression pattern of *Pygo1* and *Pygo2*

Pygo1 and Pygo2 were detected by immunofluorescence (IF) in cryosections of the developing eye. Anti-human PYGO2 antiserum (Popadiuk et al., 2006) required a relatively harsh antigen retrieval method that compromised tissue morphology but revealed Pygo2 immunoreactivity in all tissues of the eye primordium (Fig. 1E,H). *Pygo2*-null embryos served as a negative control and demonstrated labeling specificity (Fig. 1F,I). At E8.5, Pygo2 was present in the neuroepithelium of the optic pit, the neural crest-derived OM and the head surface ectoderm that includes the presumptive lens (Fig. 1E). At E9.5, Pygo2 immunoreactivity was found in the epithelia of the optic vesicle and lens placode as well as in the OM (Fig. 1H). The epithelial expression domains of Pygo2 overlapped with those of Pax6 at both E8.5 and E9.5 (Fig. 1E,G,H,J). In all cases, Pygo2 immunoreactivity appeared to be predominantly localized in the nucleus (Fig. 1E,H), although the harsh antigen retrieval method required for detection must temper this conclusion. Immunolabeling with anti-human PYGO1 antiserum (X.L., unpublished) revealed Pygo1 in the developing eye with a similar distribution to Pygo2 (data not shown).

A lens defect in *Pygo2*$^{-/-}$ has an early origin

Microophthalmia in the *Pygo2*-null mice is caused by a lens development defect. In all day-of-birth *Pygo2*$^{-/-}$ homozygotes we observed a dramatic, albeit variable, lens phenotype ranging from a small lens (Fig. 2B) to no lens (Fig. 2C). Optic cups of homozygous mutants were misshapen with abnormal retinal folds and excess mesenchymal cells (Fig. 2B,C). Lamination and differentiation of retina and retinal pigmented epithelium appeared grossly normal (Fig. 2B,C). Similar optic cup folding has been reported in other mutants with lens development defects (Ashery-Padan et al., 2000; Medina-Martinez et al., 2005; Smith et al., 2005) and is likely to be a secondary consequence of reduced lens volume.

To assess the origin of lens defects in *Pygo2*$^{-/-}$ homozygotes, we examined earlier developmental stages. To facilitate observation of the E12.5 lens in whole-mount embryos (Fig. 2D-F), we generated *Pygo2* mutant embryos incorporating the *Le-cre* transgene (Ashery-Padan et al., 2000), which has a second open reading frame for GFP and is expressed in lens (Ashery-Padan et al., 2000). This revealed that compared with control littermates (*Le-cre; Pygo2*$^{+/+}$, Fig. 2D), mutant embryos (*Le-cre; Pygo2*$^{-/-}$) show smaller (Fig. 2E) or absent (Fig. 2F) lenses. Labeling of E12.5 embryos for the lens marker β-crystallin confirmed that *Pygo2* mutants show defects ranging from a small lens (Fig. 2H) to a few β-crystallin-positive cells (Fig. 2I, arrow) or no lens at all (data not known). The consequence of the severe lens development defects for eye morphogenesis are appreciated in pigmented embryos at E12.5 where, compared with controls (Fig. 2J), *Pygo2*$^{-/-}$ mutants show pigmented epithelium that has collapsed into the center of the eye cup (Fig. 2L, arrow). These data indicate that the lens phenotype in newborn *Pygo2*$^{-/-}$ homozygotes is caused by defects in early lens development.

Pygo1 has little if any role in lens development

Pygo1 homozygotes have no detectable lens defects (data not shown). To determine whether Pygo1 might compensate for loss of Pygo2, we assessed lens size in a *Pygo1, Pygo2* allelic series in E12.5 embryos. For each genotype, we measured both eyes of at least five embryos. The data (Fig. 2K) are presented as the ratio of lens to optic cup diameter in a box plot. We used the box plot for all lens size quantification because it provides a visual representation of all the data. In a box plot, the horizontal black line is the median value, the box represents the interquartile range (25%-75% of the distribution) and the line bars the minimum and maximum values. This showed that the lens size of WT control (*Pygo1*$^{+/+}$*; Pygo2*$^{+/+}$) and *Pygo1*$^{-/-}$*; Pygo2*$^{+/-}$ embryos were not different, but that any embryo homozygous for *Pygo2* showed dramatically reduced lens size. Although combining *Pygo1* heterozygosity or homozygosity and *Pygo2* homozygosity produced a trend of smaller lenses, this was not a statistically significant change. This indicates that *Pygo1* has little role in lens development.

Pygo2 enhances placodal Pax6 expression

Pax6 has an essential, cell-autonomous function in development of the lens (Ashery-Padan et al., 2000; Collinson et al., 2000) and is sufficient to stimulate the formation of ectopic lenses if

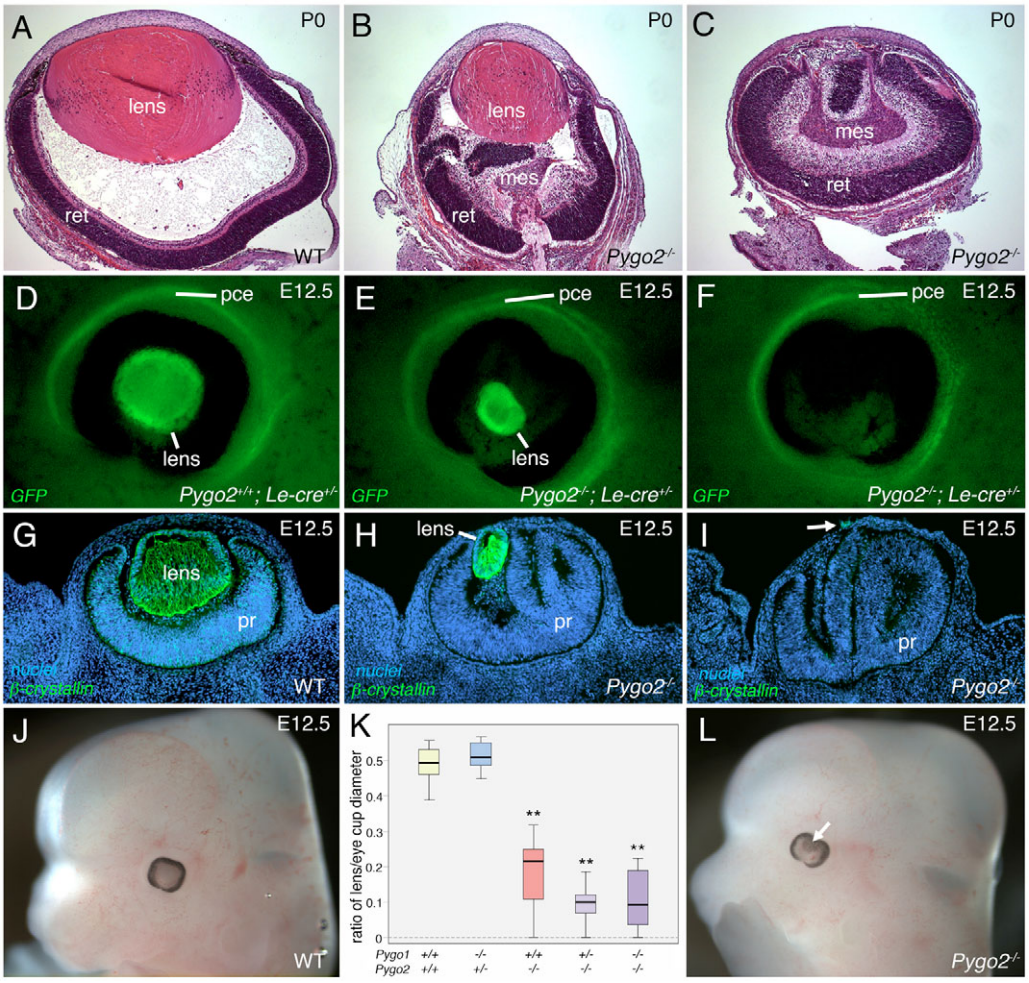

Fig. 2. *Pygo2* is required for lens development in the mouse. (**A-C**) Hematoxylin and Eosin-stained sections of eyes in wild-type (WT) and *Pygo2*$^{-/-}$ mice show mildly (B, small lens) and severely (C, no lens) affected mutants. (**D-F**) GFP fluorescence in whole-mount embryos again showing small (E) or absent (F) lenses in the mutant. (**G-I**) Eye region cryosections labeled for the lens marker *β-crystallin* (green) and for nuclei with Hoechst 33258 (blue). A small group of β-crystallin-positive cells is indicated by the arrow in I. (**J**,**L**) Whole-mount embryos showing the WT and gross *Pygo2*$^{-/-}$ phenotype. The arrow in L indicates pigmented tissue within the eye cup. (**K**) Box plot of the lens:optic cup diameter ratio in allelic series of *Pygo1* and *Pygo2* mutants. Each bar represents measurements from ten eyes in five embryos. One-way ANOVA indicated statistically significant changes as compared with the wild-type control (**, $P \leqslant 0.01 \geqslant 0$). ret, retina; mes, mesenchyme; pce, presumptive conjunctival epithelium; pr, presumptive retina.

overexpressed (Altmann et al., 1997; Chow et al., 1999). As detailed in the Introduction, models of lens induction suggest that there are two phases of Pax6 expression, of which the placodal phase (defined as *Pax6*^{placode}) is dependent on earlier Pax6 activity in the head ectoderm (defined as *Pax6*$^{pre\text{-}placode}$). Using Pax6 as a lens induction marker, we determined whether lens induction is affected in the *Pygo2*-null mice.

Pax6 expression in the head surface ectoderm was apparent in E8.5 control embryos (Fig. 3A). At E8.5, a thin layer of neural crest-derived OM separates PLE and retina (Fig. 3A). At this stage, the morphology of the eye primordium and Pax6 expression were indistinguishable between control (Fig. 3A) and *Pygo2*$^{-/-}$ homozygotes (Fig. 3B). By E9.5 in WT embryos (Fig. 3C), the optic vesicle made close contact with the surface ectoderm. As a result of inductive signaling, the surface ectoderm overlying the optic vesicle thickened to form a lens placode and this was accompanied by increased Pax6 immunoreactivity (Fig. 3C). At this stage, Pax6 expression in the optic vesicle was stronger at the edge of the forming cup (Fig. 3C). In *Pygo2*$^{-/-}$ homozygotes consistent changes were observed: the lens placode was thinner and the Pax6 expression level within placodal cells greatly reduced (Fig. 3D). There was variability in placodal Pax6 levels in the *Pygo2*$^{-/-}$ homozygotes. In some examples, Pax6 levels were moderately lower (data not shown), whereas in others there was a dramatic reduction (Fig. 3D). This is consistent with the variable lens defect apparent at later stages (Fig. 2). We observed no change in Pax6 immunoreactivity in *Pygo2*$^{+/-}$ embryos (not shown). The pattern of Pax6 immunoreactivity within the optic vesicle appeared unaffected (Fig. 3D). At E10.5, defects in eye morphogenesis became obvious in severely affected mutants: a smaller than normal lens pit formed and this structure had a lower than normal level of Pax6 expression (Fig. 3E,F).

Pax6 expression in the lens placode is regulated by both the ectoderm enhancer (EE) and other transcriptional control elements that may include the SIMO element (Kleinjan et al., 2002). In *Le-cre* transgenic mice, both Cre recombinase and GFP are expressed under control of the EE from the *Pax6* gene. *Le-cre* therefore functions as a reporter for the EE activity of *Pax6* (Ashery-Padan, 2000). To determine whether Pygo2 regulates *Pax6* transcription through the EE, we assessed GFP signal levels in *Le-cre; Pygo2*$^{-/-}$ embryos at E9.5. This showed that, compared with control *Le-cre;*

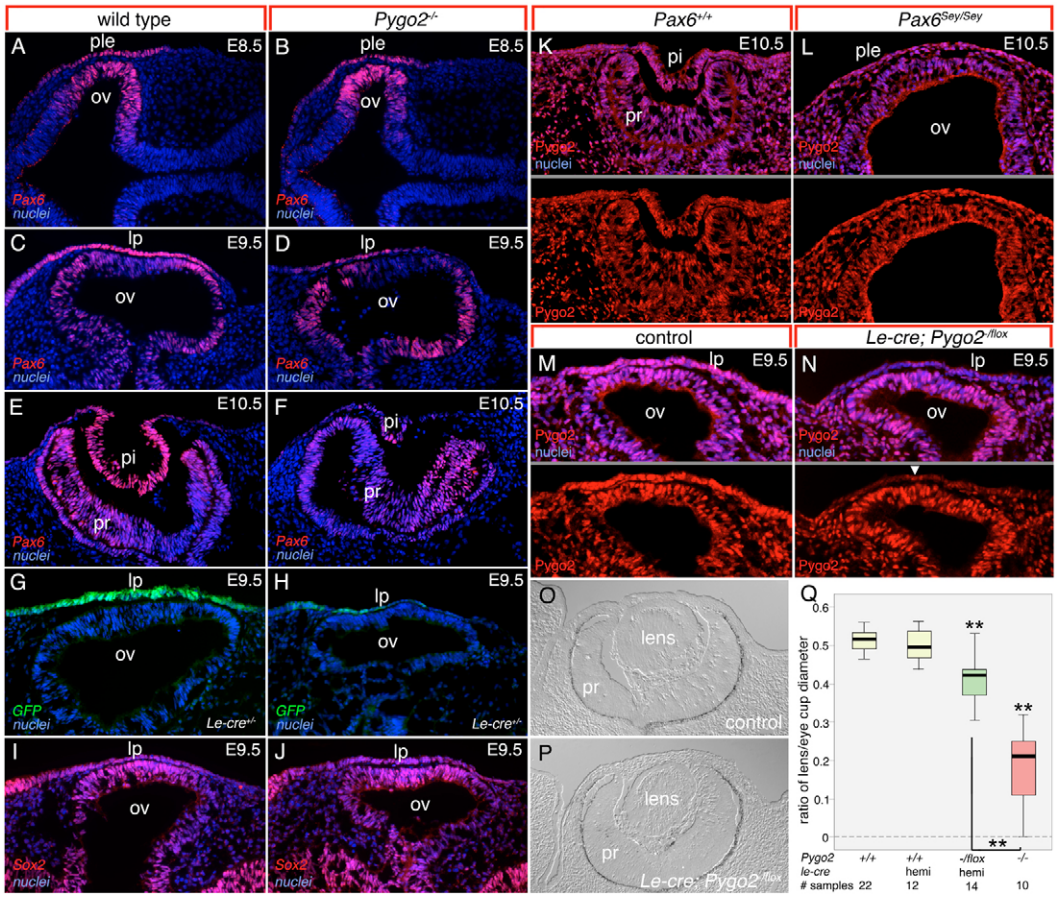

Fig. 3. Pygo2 regulates Pax6 expression in the mouse lens placode. (**A-P**) Eye region cryosections labeled for nuclei with Hoechst 33258 (A-N, blue), Pax6 (A-F, red), GFP (G,H, green), Sox2 (I,J, red), Pygo2 (K-N, red) or unlabeled differential interference contrast (DIC) images (O,P). The arrowhead in N (lower panel) indicates a small group of Pygo2-labeled cells in the presumptive lens. ple, presumptive lens ectoderm; ov, optic vesicle; lp, lens placode; pi, lens pit; pr, presumptive retina. A gray line between panels indicates that different channels of the same image are displayed. (**Q**) Box plot showing the ratio of lens to optic cup diameter in E12.5 embryos of the indicated genotypes. Mutant values (green and red bars) were significantly different (**, $P \leqslant 0.01$) from the wild-type and *Le-cre* controls (yellow bars). In addition, the *Le-cre* conditional mutant (green bar) is significantly different (**, $P \leqslant 0.01$) from the germline null (red bar). The wild-type control value incorporates the ten samples from Fig. 2K and a new set of 12 control values from this experiment which yielded the *Le-cre* conditional mutants. Germline null values are reproduced from Fig. 2K for the purposes of comparison.

Pygo2$^{+/+}$ embryos (Fig. 3G), *Le-cre; Pygo2*$^{-/-}$ embryos (Fig. 3H) had much lower levels of GFP signal. In *Pygo2*$^{-/-}$ mutants, Sox2 expression appeared unaffected (Fig. 3I,J). These data indicate that, directly or indirectly, Pygo2 regulates Pax6 expression through the EE (see model in Fig. 7D for a summary of findings).

The activity of Pygo2 regulating Pax6 expression upstream of the EE raised the possibility that Pygo2 was positioned in a pathway between the early (*Pax6*$^{pre\text{-}placode}$) and late (*Pax6*^{placode}) phases of *Pax6* expression. To test this possibility, we determined whether Pygo2 immunoreactivity was changed in *Pax6*$^{Sey/Sey}$ embryos in which *Pax6*$^{pre\text{-}placode}$ is absent. Immunolabeling in E10.5 cryosections showed no change in the level or distribution of Pygo2 (Fig. 3K,L), even though eye development was arrested. This suggests that *Pygo2* functions in parallel to *Pax6*$^{pre\text{-}placode}$ in regulating *Pax6* expression through the EE (Fig. 7D).

Pygo2 functions cell autonomously in lens induction

Pygo2 expression in all components of the eye primordium raised the question of which expression domains might be crucial for lens development. We generated conditional *Pygo2* mutants using Cre recombinase transgenes that were expressed in different components of the early eye. The expression patterns of these Cre transgenes are summarized in Fig. 7C. As mentioned, the *Le-cre* transgene relies on the EE from *Pax6* for expression in the PLE from E8.75 onwards.

Using anti-Pygo2 antibodies, we showed that in *Le-cre; Pygo2*$^{flox/-}$ embryos, Pygo2 was consistently lost from the E9.5 lens placode (Fig. 3M,N). In some cases, we detected a few Pygo2-positive placodal cells (Fig. 3N, arrowhead). At E10.5, Pygo2 immunoreactivity was absent from the mutant lens pit (data not shown). To assess phenotype severity in *Le-cre; Pygo2*$^{flox/-}$ embryos, we quantified lens size at E12.5 (Fig. 3O-Q). This showed that despite consistent evidence of *Pygo2*^{flox} deletion with *Le-cre*, E12.5 lens size was only mildly reduced, as compared with either WT or *Le-cre* embryos, and did not reach the severity of the null (Fig. 3Q). This indicates that Pygo2 has a cell-autonomous function in lens development but also implies that additional Pygo2-expressing domains contribute.

Mesenchymal Pygo2 has a cell non-autonomous role in lens induction

To assess the role of mesenchymal *Pygo2* in lens development we generated mice in which *Pygo2*^{flox} was deleted with the *Wnt1-cre* driver (Danielian et al., 1998). The *Wnt1* gene is expressed in the region of dorsal neural tube that is the origin of neural crest, and can be used to conditionally delete floxed alleles in the neural crest-derived OM. This can be demonstrated using the *Z/EG* GFP reporter mouse (Novak et al., 2000) in conjunction with *Wnt1-cre* at both E8.5 (Fig. 4A,B) and E9.5 (Fig. 4C,D), OM cells are GFP positive. This includes the narrow band of mesenchyme separating presumptive lens and retinal epithelia at E8.5 (Fig. 4B), as well as mesenchyme adjacent to the optic vesicle after epithelial contact at E9.5 (Fig. 4D). GFP-positive cells also label for the transcription factor Ap2α (Tcfap2a – Mouse Genome Informatics), a marker of both PLE and OM (Zhang et al., 1996; Nottoli et al., 1998) (Fig. 4B,D).

Immunolabeling showed that the OM of *Wnt1-cre, Pygo2*$^{flox/-}$ embryos is Pygo2 negative (Fig. 4E,F). Small clusters of cells within the periocular region that remained Pygo2 positive correspond to blood vessels (Fig. 4F, arrows) that are not derived from *Wnt1-cre*-expressing cells (Fig. 4D, asterisks). Quantification of lens size in *Wnt1-cre; Pygo2*$^{flox/-}$ embryos at E12.5 (Fig. 4G-J) revealed a mild reduction approximately as severe as the phenotype in *Le-cre; Pygo2*$^{flox/-}$ embryos (Fig. 5O). Consistent with this mild phenotype, we observed a slight reduction in the levels of Pax6 immunoreactivity in the lens placode of *Wnt1-cre; Pygo2*$^{flox/-}$ embryos (Fig. 4K-N). Though consistently observed, this reduction could be subtle and was best detected in double-labeled samples in which Ap2α immunoreactivity served as an unchanging internal control (Fig. 4K,L, red). Detection of Pax6 in the overlaid red channel gave most placodal nuclei a yellow color (Fig. 4K,L). Where Pax6 expression levels were reduced – in the temporal one third of the placodal ectoderm – there was a 'red-shift' (Fig. 4L, bracket). These changes can be detected in the color intensities across line intervals through the lens placode (Fig. 4M,N). Reduced Pax6 labeling levels can be quantified by representing Pax6 and Ap2α average labeling intensities across the placodal line interval as a ratio (Fig. 5P; see Materials and methods for details). These data indicate that mesenchymal Pygo2 participates in lens development by regulating placodal Pax6 expression, either through mesenchymal-epithelial signaling or by enhancing the lens-inducing capacity of the optic vesicle. As with *Le-cre* conditional mutants, the severity of the *Wnt1-cre; Pygo2*$^{flox/-}$ phenotype did not match that of the null (Fig. 5O).

Pygo2 in PLE and OM combine to regulate Pax6 and lens development

With the above data, we reasoned that the severe lens phenotype in the *Pygo2*-null mutant might be reconstructed by conditional deletion of *Pygo2* in both PLE and OM. We compared two strategies for conditional deletion. First, we simply combined the *Le-cre* and *Wnt1-cre* drivers with *Pygo2*$^{flox/-}$ and determined the severity of the lens phenotype. This showed that although the phenotype (data not shown) was more severe (Fig. 5O), the dramatic phenotype of the *Pygo2*-null was not reproduced.

As a second strategy for conditional deletion of *Pygo2* in both presumptive lens and OM, we employed the *Ap2α-cre* mouse line (Macatee et al., 2003). In this line, Cre recombinase is expressed from the endogenous *Ap2α* locus. Since this was generated via insertion of an internal ribosome entry sequence and *cre* into the 3′ untranslated region of *Ap2α*, production of Ap2α should be unaffected (Macatee et al., 2003). The advantage of using *Ap2α-cre* compared with the *Wnt1-cre, Le-cre* combination is that *Ap2α-cre* is expressed throughout the head surface ectoderm of the mouse from approximately E8.0 (Fig. 7C). This precedes *Le-cre* expression in ectoderm by nearly 24 hours and so allows us to determine whether expression of Pygo2 in this domain might be crucial.

Generation of *Ap2α-cre; Z/EG* embryos indicated that, as anticipated (Macatee et al., 2003), GFP-positive cells are found in the head surface ectoderm and OM at E8.5 (Fig. 5A,B), as well as in the lens placode and OM at E9.5 (Fig. 5C,D). Pygo2 labeling of cryosections from *Ap2α-cre; Pygo2*$^{flox/-}$ embryos revealed that Pygo2 immunoreactivity was absent from both presumptive lens and OM at E9.5 (Fig. 5A,B), indicating that *Ap2α-cre* was effective. Although the E12.5 lens phenotype in *Ap2α-cre; Pygo2*$^{flox/-}$ embryos was the most severe of any of the conditional deletion mutants, it still did not reach the severity of the null. This could be observed in whole-mount embryos (Fig. 5G,I) and in eye region sections of whole mounts (Fig. 5H,J), and was apparent from lens size quantification (Fig. 5O). This quantification indicates that the phenotype severity in *Ap2α-cre; Pygo2*$^{flox/-}$ embryos is greater than in the *Le-cre; Wnt1-cre; Pygo2*$^{flox/-}$ (a statistical trend) or in either of the single Cre-driver mutants (statistically significant). Combined, these data indicate that Pygo2 in pre-placodal ectoderm, in lens placode and in OM, all participate in lens development cooperatively.

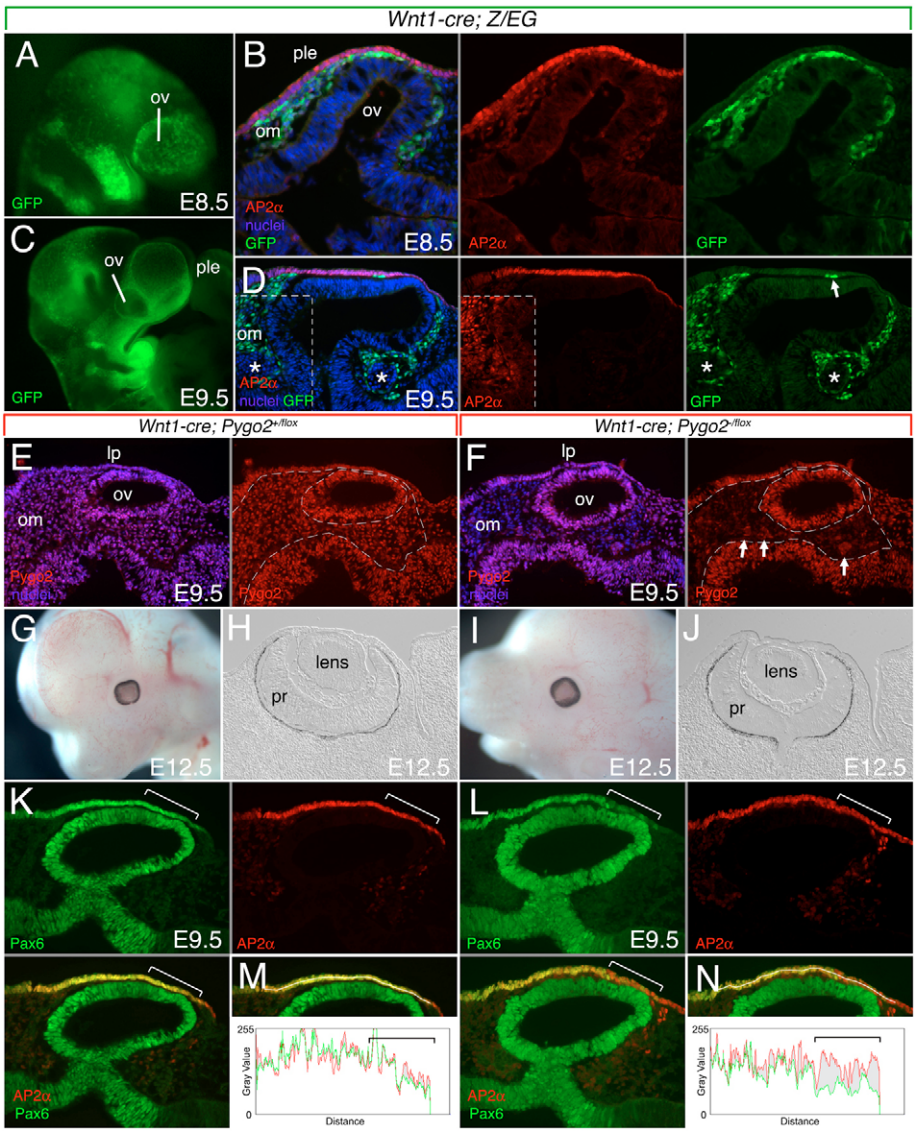

Fig. 4. Mesenchymal Pygo2 participates in lens development. (**A**,**C**,**G**,**I**) Whole-mount mouse embryos visualized for GFP (A,C) or in bright-field (G,I). (**B**,**D-F**,**H**,**J-N**) Unlabeled, DIC-illuminated cryosections (H,J), and cryosections labeled for nuclei with Hoechst 33258 (B,D-F, blue), Ap2α (B,D,K-N, red), GFP (B,D, green), Pygo2 (E,F, red) or Pax6 (K-N, green). A gray line between panels indicates that different channels of the same image are displayed. In D, the red channel within the dashed box has been enhanced to show weak Ap2α immunoreactivity in the ocular mesenchyme, the asterisks indicate GFP-negative blood vessels, and the arrow indicates remaining mesenchymal cells between presumptive lens and retinal epithelia. In E,F, the dashed line encloses approximately equivalent regions of the OM. In F, arrows point to Pygo2-positive blood vessels. In M,N are shown the green (Pax6) and red (Ap2α) channel intensities for a line interval passing through the nuclei of the lens placode. The bracket indicates the regions in the lens placode with a reduced Pax6:Ap2α ratio in the *Pygo2* mutant. ple, presumptive lens ectoderm; ov, optic vesicle; om, ocular mesenchyme; lp, lens placode; pr, presumptive retina.

Importantly, we observed a reduced level of Pax6 expression in the E9.5 lens placode of *Ap2α-cre; Pygo2*$^{flox/-}$ embryos (Fig. 5K-N). As described above, this change was easiest to observe when Pax6 labeling (Fig. 5K,L, green) was overlaid with Ap2α labeling (Fig. 5K,L, red). As described in Materials and methods, reduced Pax6 labeling levels can be quantified (Fig. 5P). Notably, the Pax6:Ap2α ratio was lower in the *Ap2α-cre* than *Wnt1-cre* conditional, and higher than in the germline null. This is entirely consistent with the severity of the E12.5 lens size phenotype in each mutant (Fig. 5O) and with a cooperative action of ectodermal and OM Pygo2 in lens development. By elimination, we anticipate that combined conditional deletion of *Pygo2*^{flox} in presumptive lens, OM and optic vesicle, would result in reconstruction of the null phenotype.

Mesenchymal Pygo2 modulates lens development independent of its activity in Wnt signaling

In *Drosophila*, Pygopus functions in the Wnt pathway (Belenkaya et al., 2002; Kramps et al., 2002; Parker et al., 2002; Thompson et al., 2002). Thus, we considered the possibility that defective Wnt signaling in the early eye could result in the failure of Pax6 upregulation and of lens development. A number of *lacZ*-based Wnt pathway reporter transgenic mouse lines have been developed including *TOPGAL* (DasGupta and Fuchs, 1999), *BatGAL* (Maretto et al., 2003) and *BatlacZ* (Nakaya et al., 2005). These reporter lines have been used to examine the pattern of Wnt-responsive cells in the developing eye (Liu et al., 2003; Smith et al., 2005). The patterns of expression of these reporters are not identical, but analysis revealed that at E8.5, the neural crest-derived OM is a prominent location of both *TOPGAL* (data not shown) and *BatlacZ* (Fig. 6A,C,E) expression. By contrast, PLE was negative at E8.5 (Fig. 6A,C,E) and E9.5 (data not shown) for both *TOPGAL* (data not shown) and *BatlacZ* (Fig. 6A,C,E). This is consistent with a previous report (Smith et al., 2005) suggesting that Wnt signaling must be absent from the ectoderm if lens development is to proceed.

To validate the *BatlacZ* reporter results for cells of the OM, we performed *β-catenin* loss- and gain-of-function experiments using the *Wnt1-cre* driver. In litters of E8.5 embryos that showed *BatlacZ* expression in the OM, littermates with the OM-specific *β-catenin* gain-of-function genotype *BatlacZ; Wnt1-cre; Catnb*$^{+/lox(ex3)}$ showed dramatically enhanced *lacZ* staining of OM cells (Fig. 6A,B). By contrast, in embryos with the *β-catenin* loss-of-function

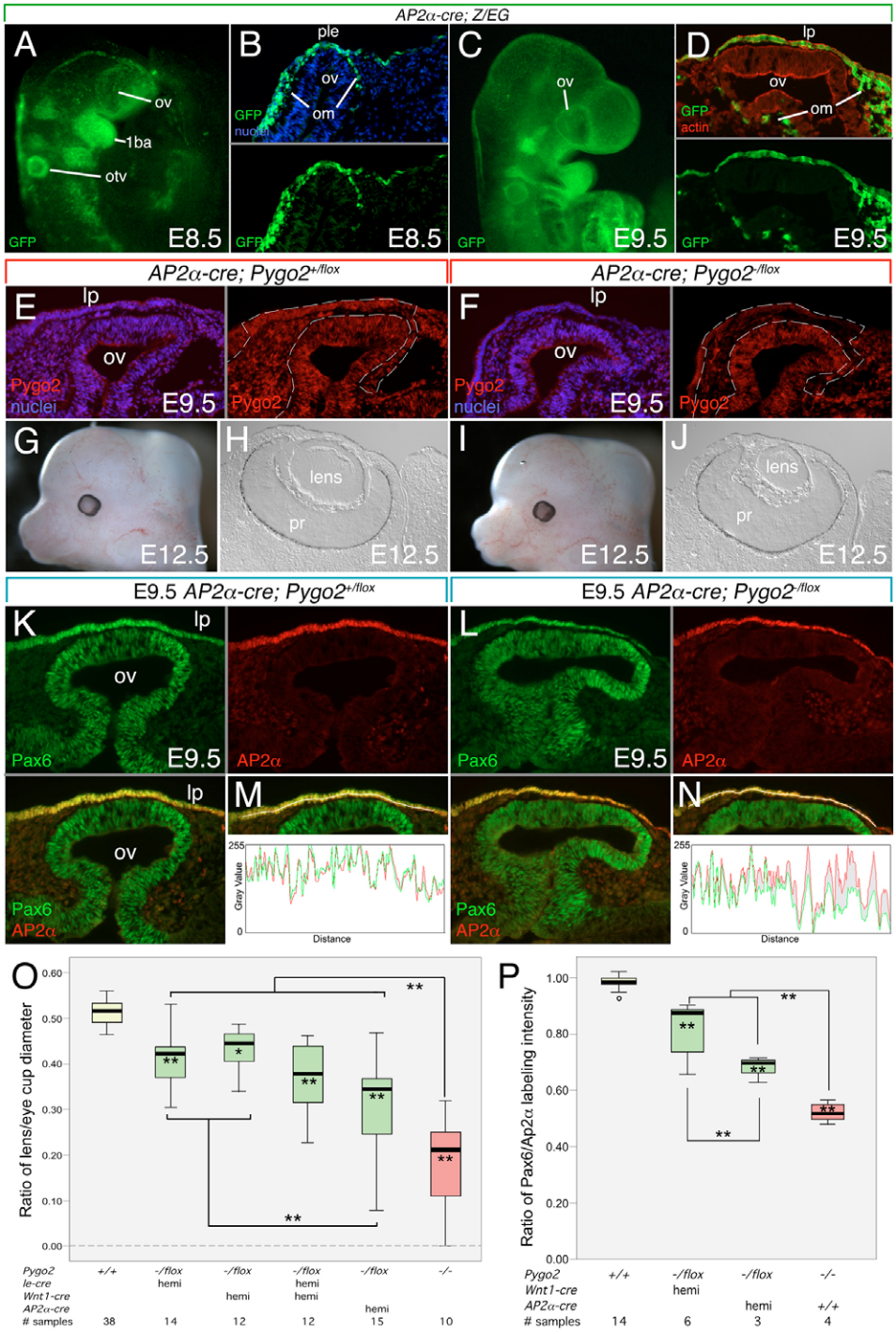

Fig. 5. Mesenchymal and ectodermal Pygo2 cooperate in mouse lens development. (**A**,**C**,**G**,**I**) Whole-mount embryos unstained (G,I) or visualized for GFP (A,C). (**B**,**D-F**,**H**,**J**,**K-N**) Unlabeled, DIC-illuminated cryosections (H,J) and cryosections labeled for nuclei (B,E,F, blue), GFP (B,D, green), F-actin (D, red), Pygo2 (E,F, red), Pax6 (K-N, green) and Ap2α (K-N, red). In E,F, the dashed line encloses approximately equivalent regions of mesenchyme and surface ectoderm. In M,N are shown the green (Pax6) and red (Ap2α) channel intensities for a line interval passing through the nuclei of the lens placode. ov, optic vesicle; 1ba, first branchial arch; otv, otic vesicle; ple, presumptive lens ectoderm; om, ocular mesenchyme; lp, lens placode; pr, presumptive retina. A gray line between panels indicates that different channels of the same image are displayed. (**O**) Box plot showing the ratio of lens to optic cup diameter in E12.5 embryos of the indicated genotypes. Mutant values (green and red bars) were significantly different from the wild-type control (yellow bar); * within the box, $P \leqslant 0.05 > 0.01$ (*Wnt1-cre*); ** within the box, $P \leqslant 0.01 \geqslant 0$ (*Le-cre*, *Le-cre; Wnt1-cre* double, *Ap2α-cre*, germline null). Conditional mutant values (green bars) were significantly different (**, $P \leqslant 0.01 \geqslant 0$) from the germline null (red bar). *Wnt1-cre* and *Le-cre* conditional mutants were also significantly different (**, $P \leqslant 0.01 \geqslant 0$) from the *Ap2α-cre* conditional mutant. (**P**) Box plot showing the ratio of average Pax6:Ap2α labeling intensity across the lens placode (as in Fig. 4M,N and Fig. 5M,N) for the genotypes indicated. Mutant values (green and red bars) were significantly different from the wild-type control (yellow bar); ** within the box, $P \leqslant 0.001 \geqslant 0$). Conditional mutant values (green bars) were significantly different (** within the box, $P \leqslant 0.001 \geqslant 0$) from the germline null (red bar). *Wnt1-cre* conditional mutants were also significantly different (** within the box, $P \leqslant 0.001 \geqslant 0$) from the *Ap2α-cre* conditional mutants.

genotype *BatlacZ; Wnt1-cre; Catnb*$^{tm2Kem/tm2Kem}$, *lacZ* staining was absent from the OM (Fig. 6C,D). These data show that *BatlacZ* can be used as a model Wnt pathway target gene in the OM.

To determine whether Pygo2 might function within the Wnt pathway, we first generated *BatlacZ; Pygo2*$^{-/-}$ embryos and found reduced levels of OM *lacZ* staining (Fig. 6E,F). To determine whether this was a cell-autonomous Wnt pathway response, we also generated *BatlacZ; Wnt1-cre; Pygo2*$^{flox/-}$ embryos and counted *lacZ*-positive cells in these and the germline null. Cell counting was performed on sections for different regions of E8.5 embryos, including the *lacZ*-positive OM, optic vesicle and the dorsal neural tube in the areas indicated (Fig. 6E, colored dashed lines). This analysis showed that in both the germline null and the OM-specific deletion, the number of *lacZ*-labeled OM cells was reduced (Fig. 7A). In the germline null mutant, reduced numbers of *BatlacZ*-expressing cells in the dorsal neural tube (Fig. 7A) served as an internal control. In neither the germline nor conditional nulls did the total number of OM cells or the number of optic vesicle *lacZ*-positive cells change (Fig. 7A). Combined, the data from Figs 6 and 7 show that both Pygo2 and β-catenin can regulate a model Wnt pathway target gene.

If the OM activity of Pygo2 in lens development is a Wnt pathway function then we would expect deletion of Pygo2 or β-catenin in OM cells to produce similar lens development defects. We generated *Wnt1-cre; Catnb*$^{tm2Kem/tm2Kem}$ embryos and showed that β-catenin immunoreactivity was absent from the OM at E9.5 (Fig. 6G,H) and that, as shown earlier (Fig. 6A,B), when *BatlacZ* was incorporated the response was absent at E8.5. Interestingly, unlike the OM-conditional deletion of *Pygo2* where placodal Pax6 levels were reduced (Fig. 4K-N, Fig. 5P), the level of placodal Pax6 with OM-conditional deletion of *β-catenin* was unchanged (Fig. 6G,H, green). As a second measure of lens development, we allowed some litters to progress until E12.5 (Fig. 6I-L) and quantified lens size (Fig. 7B). This showed that in contrast to OM deletion of *Pygo2* where lens size is reduced (Fig. 7B), loss of β-catenin in the OM had no effect (Fig. 7B). Since there is no possibility of Wnt pathway function in the OM in the absence of β-catenin, this suggests that although Pygo2 can regulate a model Wnt pathway target gene, its function in lens development is independent of Wnt pathway activity.

DISCUSSION

We have investigated the function of *Pygo2* in lens development. We show that Pygo2 functions at the inductive phases of lens development and that there is no apparent cooperative activity with Pygo1. Pygo2 is expressed ubiquitously in tissues of the early eye, including the optic vesicle, OM and presumptive lens. Conditional deletion of *Pygo2* using a selection of Cre drivers showed that Pygo2 activity in multiple tissues contributes to lens development. Below, we consider three issues that arise from this analysis.

In which signaling pathways does Pygo2 function during lens development?

Drosophila Pygopus was identified as a core component of the Wingless pathway (Belenkaya et al., 2002; Kramps et al., 2002; Parker et al., 2002). Pygopus has been shown to interact directly with Armadillo/β-catenin in the nucleus and to regulate transcription of Wingless target genes (Thompson, 2004; Tolwinski and Wieschaus, 2004; Townsley et al., 2004; Hoffmans et al., 2005; Stadeli and Basler, 2005). Analysis in *Xenopus* has shown that Pygopus is required for Wnt signaling in a vertebrate (Belenkaya et al., 2002; Lake and Kao, 2003). In *Drosophila*, *pygopus* loss-of-function phenocopies Wg pathway defects (Belenkaya et al., 2002; Parker et al., 2002; Thompson et al., 2002). In the mouse, general Wnt pathway loss-of-function (for example in the *Lrp6* mutant mouse) (Pinson et al., 2000) also results in severe, mid-gestational developmental defects. Here we show the contrasting result that deletion of *Pygo1* and *Pygo2* in the mouse results in a relatively mild phenotype distinct from Wnt pathway loss-of-function.

During early eye development, there are multiple roles for the Wnt pathway. In zebrafish, the Wnt pathway antagonizes eye specification as a step in defining eye fields (Cavodeassi et al., 2005). Later, when the basic components of the eye are formed, Wnt pathway responses serve to restrict the domain of surface ectoderm that can form lens; compromising Wnt signaling in surface ectoderm results in the formation of ectopic lentoid bodies (Smith et al., 2005). This activity might be analogous to the function of the Wingless pathway in the fly, where it suppresses formation of eye in favor of head cuticle (Treisman and Rubin, 1995). The phenotype of the *Lrp6* mutant mouse also implies that Wnt signaling has an important function in maintaining the lens epithelium during later lens development (Stump et al., 2003).

Here we show that the neural crest-derived OM is Wnt pathway responsive. In the mouse, a layer of OM a few cells thick separates the presumptive lens and retinal epithelia from approximately E8.0 until E9.0, when the distal epithelium of the optic vesicle makes close contact with the presumptive lens (Kaufman, 1992). Throughout this period, the OM expresses both the validated Wnt reporter *BatlacZ* (Nakaya et al., 2005) and *TOPGAL* (DasGupta and Fuchs, 1999). When combined with the observation that *BatlacZ* expression is reduced upon OM-conditional *Pygo2* deletion, we conclude, as might be anticipated (Belenkaya et al., 2002; Kramps et al., 2002; Parker et al., 2002; Thompson, 2004; Tolwinski and Wieschaus, 2004; Townsley et al., 2004; Hoffmans et al., 2005; Stadeli and Basler, 2005) that Pygo2 has a Wnt pathway function.

However, Wnt pathway activity of Pygo2 is apparently not required for its role in lens development. Assessing lens development in the mesenchyme-specific conditional deletion of *Pygo2* showed that the crucial lens development marker Pax6 is reduced in the PLE and that by E12.5 the lens is small. By contrast, conditional deletion of *β-catenin* in the OM had no impact on Pax6 levels in PLE, nor on lens size at E12.5. A comparison of the consequences of OM deletion of *Pygo2* and *β-catenin* for lens development indicates that although Pygo2 can function in the Wnt pathway, this activity is not important for lens development. By inference, mesenchymal Pygo2 must function in another pathway to influence lens development. Similarly, the absence of a Wnt pathway response in the lens placode, but a role for placodal Pygo2 in lens development, suggests a non-Wnt pathway function in this tissue as well. These conclusions are consistent with non-Wnt pathway functions for *Drosophila* Pygopus (Belenkaya et al., 2002; Parker et al., 2002). Like *Drosophila* Pygopus, mouse Pygo2 is expressed more broadly than the locations of Wnt pathway activity (Parker et al., 2002; Li et al., 2004).

In the mouse, Pygo2 in OM enhances development of the lens

Embryological manipulations have indicated that neural crest-derived OM suppresses lens formation and is important in determining where and when a lens can form. In the chick, culture of isolated head ectoderm results in an expanded expression domain of the lens marker δ-crystallin; recombining head ectoderm with head mesenchyme suppresses this response (Sullivan et al., 2004). Mesenchymal suppression of lens fate might also explain much earlier studies in which removal of neural

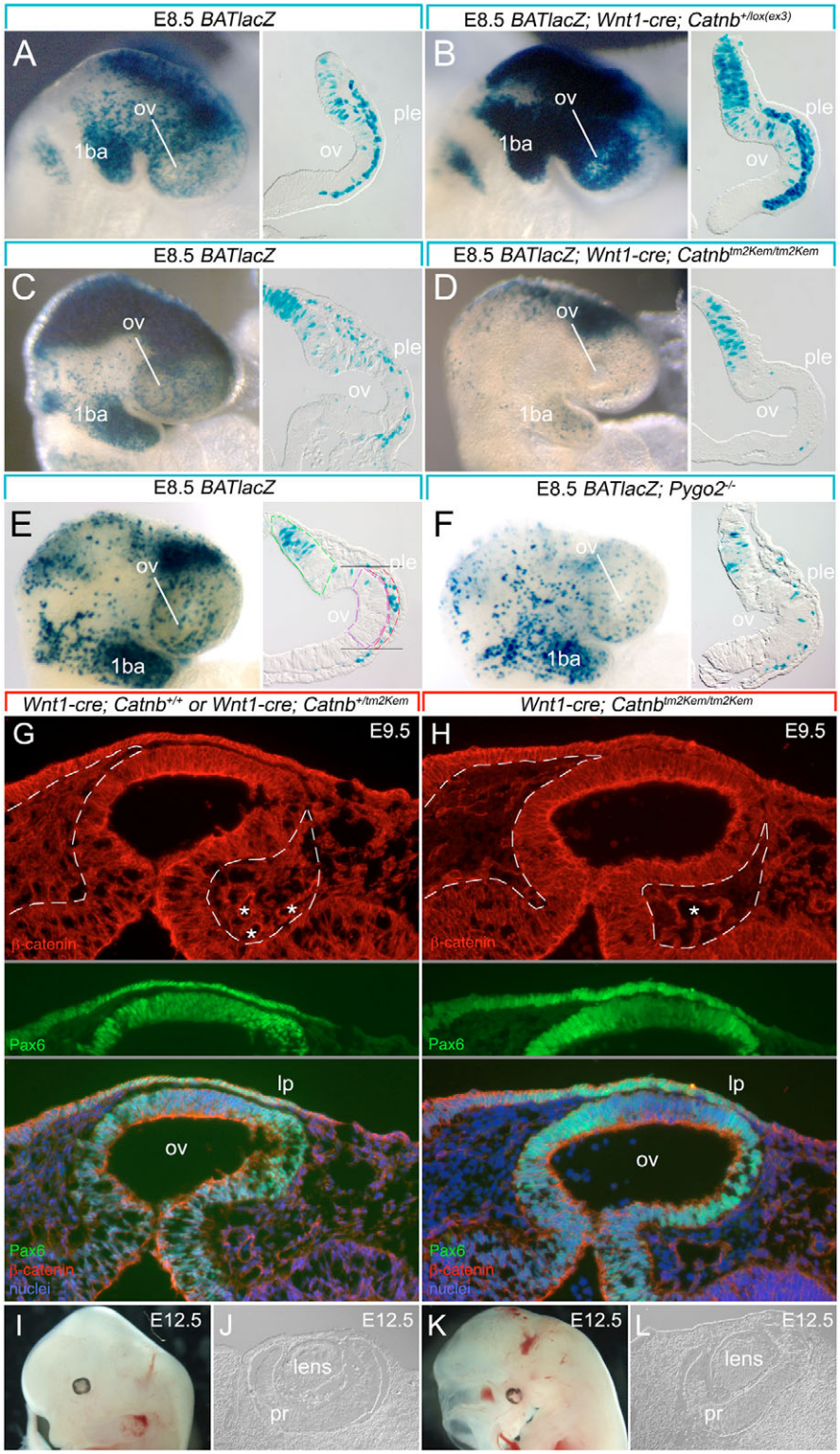

Fig. 6. β-catenin/Wnt signaling in the OM is not required for lens development. (**A-F**) Whole-mount mouse embryo heads and eye region sections stained for β-gal activity. The section shown in E defines the regions where quantification was performed for Fig. 7A. Dashed green line, dorsal neural tube (DNT); dashed purple line, optic vesicle (OV); dashed red line, ocular mesenchyme (OM). (**G**,**H**) Cryosections labeled for β-catenin (red), Pax6 (green) and nuclei (blue). The dashed lines enclose regions of OM negative for β-catenin immunoreactivity. Asterisks indicate blood vessels that remain immunoreactive to β-catenin. (**I-L**) Whole-mount (I,K) and DIC-illuminated eye region sections (J,L). ov, optic vesicle; 1ba, first branchial arch; ple, presumptive lens ectoderm; om, ocular mesenchyme; lp, lens placode; pr, presumptive retina. A gray line between panels indicates that different channels of the same image are displayed.

plate regions resulted in formation of ectopic lenses (von Woellwarth, 1961). In the chick, neural crest-derived head mesenchyme has been clearly identified as the lens-suppressive population (Bailey et al., 2006). This is dramatically illustrated by the formation of an ectopic lens when the neural folds are removed. This ectopic lens forms in a region of ectoderm posterior to the eye (Bailey et al., 2006) that in the mouse corresponds to a domain where the *Pax6* EE is active (Williams et al., 1998; Dimanlig et al., 2001). Though this study implicates Fgf signaling in promoting the identity of other placodal structures in ectoderm previously specified for lens, the identity of mesenchymal signals that directly suppress lens formation is unclear.

Our analysis of the influence of mesenchymal Pygo2 on lens development makes an interesting comparison. Mesenchymal deletion of *Pygo2* (using *Wnt1-cre*, Fig. 7C) results in a lower level of Pax6 in a sub-region of the lens placode and in an E12.5 lens that

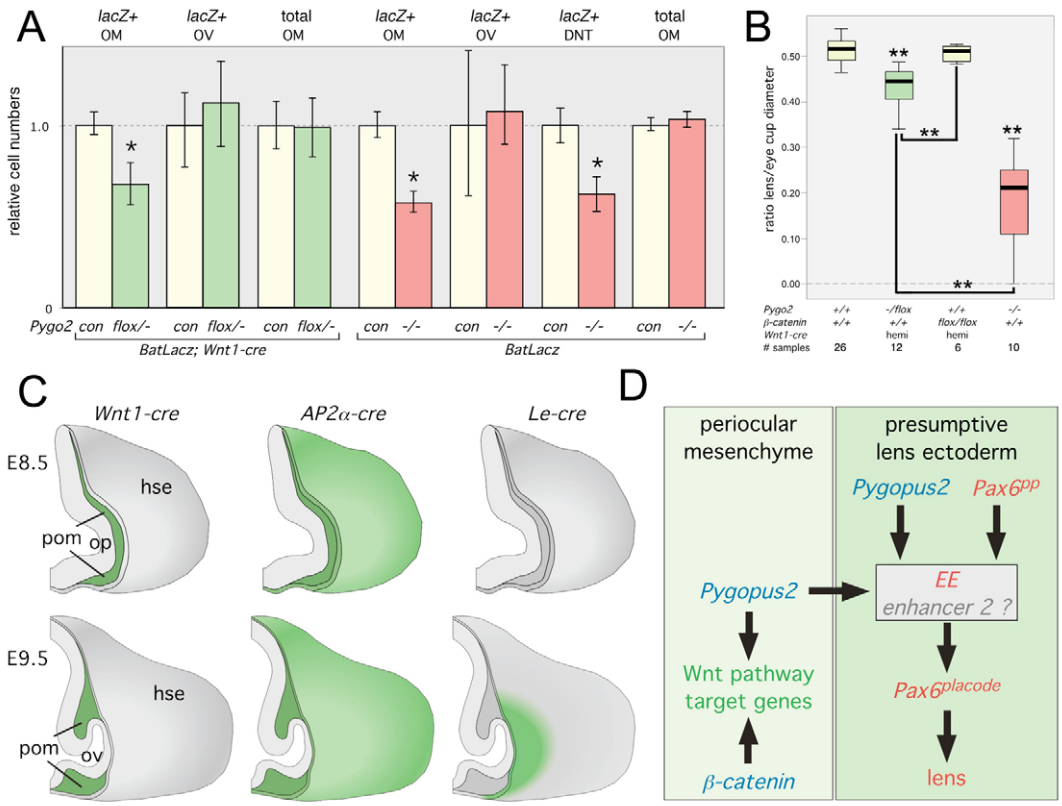

Fig. 7. Wnt-independent function of mesenchymal Pygo2 in lens development. (**A**) Quantification of *lacZ*-positive cells or total cells relative to control in the ocular mesenchyme of E8.5 mouse embryos of the indicated genotypes. The regions quantified are shown in Fig. 6E. *, $P \leqslant 0.05 > 0.01$. (**B**) Box plot showing the ratio of lens to optic cup diameter in E12.5 embryos of the indicated genotypes. **, $P \leqslant 0.01 \geqslant 0$. The wild-type control value incorporates the ten samples from Fig. 2K, 12 samples from the Fig. 3Q experiment that yielded the *Wnt1-cre* conditional mutants and a new set of four control values from this experiment that yielded the *Wnt1-cre; β-catenin* conditional mutants. The germline null and *Wnt1-cre* conditional null values are reproduced from Fig. 2K and Fig. 5O, respectively, for the purposes of comparison. (**C**) Summary of cre expression patterns. Schematic of the right-hand side of E8.5 (top row) and E9.5 (bottom row) mouse embryos anterior to the midpoint of the optic vesicle. The green regions indicate the tissue domains in which the listed Cre drivers can perform allele conversions. om, ocular mesenchyme; op, optic pit; ov, optic vesicle; hse, head surface ectoderm. (**D**) Model for the involvement of Pygo2 in lens development (see text for details). $Pax6^{pp}$ represents $Pax6^{pre\text{-}placode}$.

has, on average, a 14% reduction in diameter. Thus, Pygo2 in neural crest-derived OM has a positive influence on lens development. So far, we have not found any indication of ectopic lens formation with OM-conditional mutation of *Pygo2*. Thus, neither the Wnt nor the non-Wnt activities of Pygo2 are essential for neural-crest suppression of lens formation. This is consistent with preliminary experiments in the chick (Bailey et al., 2006) suggesting that Wnt ligands do not suppress formation of ectopic lenses arising in the absence of neural crest. Since ectopic lenses form nasal to the eye when *β-catenin* is deleted from surface ectoderm in the mouse (Smith et al., 2005), we conclude that there may be multiple mechanisms for suppression of lens formation.

A model for Pygo2 involvement in lens induction

We propose a model for the function of Pygo2 in development of the lens (Fig. 7D). This is primarily a genetic model but can be superimposed on the tissue structures to indicate likely tissue interactions. In $Pygo2^{-/-}$ embryos, reduced Pax6 IF and *Le-cre(GFP)* reporter expression suggest that *Pygo2* is upstream of the EE in regulating the placodal phase of Pax6 expression (Fig. 7D). By contrast, in the *Pygo2* germline null, the pre-placodal phase of Pax6 expression (head surface ectoderm) is unchanged. In a reciprocal experiment, we showed that in $Pax6^{Sey/Sey}$ embryos (which represent the pre-placodal phase of *Pax6*), Pygo2 expression was unchanged. These data argue for a genetic model in which *Pygo2* and $Pax6^{pre\text{-}placode}$ converge on the EE to regulate *Pax6* expression. Previous analysis has shown that $Pax6^{placode}$ depends on the EE and at least one additional enhancer (Dimanlig et al., 2001). With the information currently available, we cannot exclude the involvement of another *Pax6* lens enhancer in Pygo2-dependent regulation. The best candidate for a second lens enhancer in *Pax6* is the SIMO element (Kleinjan et al., 2001). It has been suggested that Pax6 can directly bind the EE (Aota et al., 2003). Pygo2 influence on the EE could be direct or indirect.

Regional deletion of the *Pygo2* conditional allele has indicated that Pygo2 in multiple tissues contributes to lens development. Deletion of $Pygo2^{flox}$ with *Wnt1-cre* (Danielian et al., 1998) (Fig. 7C) indicates that Pygo2 in neural crest-derived OM positively influences lens development. In one model, this could occur by direct signaling of OM to presumptive lens (Fig. 7D) or, conceivably, indirectly through enhancement of the ability of the optic vesicle to induce lens. Either way, the end result is Pygo2-dependent upregulation of $Pax6^{placode}$. The more-severe lens phenotype occurring when *Wnt1-cre* is combined with the post-

induction placodal ectoderm-driver *Le-cre* (Fig. 7C) indicates that mesenchymal and placodal *Pygo2* cooperate (Fig. 7D). A comparison of that outcome with the *Ap2α-cre* conditional (where deletion also occurs in pre-placodal ectoderm, Fig. 7C) suggests that this domain is also involved. This is consistent with a function for *Pygo2* in parallel with *Pax6*$^{pre\text{-}placode}$ (Fig. 7D). It is interesting to note that *Pygo2* influences lens development through the EE, as do both Fgf receptor and Bmp7 signaling (Lang, 2004). It will be interesting to determine whether the non-Wnt activity of Pygo2 resides in one of these pathways.

We thank Paul Speeg and Lucas McClain for excellent technical assistance; Drs Andras Nagy and Alex Kuan for *Z/EG* and Dr Mark Taketo for the *β-catenin* gain-of-function mice. The R.A.L. laboratory is supported by NIH RO1s EY16241, EY14102, EY15766, NIH RO3 EY14826 and by funds from the Abrahamson Pediatric Eye Institute Endowment at the Children's Hospital Medical Center of Cincinnati.

References

Altmann, C. R., Chow, R. L., Lang, R. A. and Hemmati-Brivanlou, A. (1997). Lens induction by Pax-6 in Xenopus laevis. *Dev. Biol.* **185**, 119-123.

Aota, S., Nakajima, N., Sakamoto, R., Watanabe, S., Ibaraki, N. and Okazaki, K. (2003). Pax6 autoregulation mediated by direct interaction of Pax6 protein with the head surface ectoderm-specific enhancer of the mouse Pax6 gene. *Dev. Biol.* **257**, 1-13.

Ashery-Padan, R., Marquardt, T., Zhou, X. and Gruss, P. (2000). Pax6 activity in the lens primordium is required for lens formation and for correct placement of a single retina in the eye. *Genes Dev.* **14**, 2701-2711.

Bailey, A. P., Bhattacharyya, S., Bronner-Fraser, M. and Streit, A. (2006). Lens specification is the ground state of all sensory placodes, from which FGF promotes olfactory identity. *Dev. Cell* **11**, 505-517.

Belenkaya, T. Y., Han, C., Standley, H. J., Lin, X., Houston, D. W. and Heasman, J. (2002). pygopus Encodes a nuclear protein essential for wingless/Wnt signaling. *Development* **129**, 4089-4101.

Bell, S. M., Schreiner, C. M., Waclaw, R. R., Campbell, K., Potter, S. S. and Scott, W. J. (2003). Sp8 is crucial for limb outgrowth and neuropore closure. *Proc. Natl. Acad. Sci. USA* **100**, 12195-12200.

Brault, V., Moore, R., Kutsch, S., Ishibashi, M., Rowitch, D. H., McMahon, A. P., Sommer, L., Boussadia, O. and Kemler, R. (2001). Inactivation of the beta-catenin gene by Wnt1-Cre-mediated deletion results in dramatic brain malformation and failure of craniofacial development. *Development* **128**, 1253-1264.

Cavodeassi, F., Carreira-Barbosa, F., Young, R. M., Concha, M. L., Allende, M. L., Houart, C., Tada, M. and Wilson, S. W. (2005). Early stages of zebrafish eye formation require the coordinated activity of Wnt11, Fz5, and the Wnt/beta-catenin pathway. *Neuron* **47**, 43-56.

Chow, R. L., Altmann, C. R., Lang, R. A. and Hemmati-Brivanlou, A. (1999). Pax6 induces ectopic eyes in a vertebrate. *Development* **126**, 4213-4222.

Collinson, J. M., Hill, R. E. and West, J. D. (2000). Different roles for Pax6 in the optic vesicle and facial epithelium mediate early morphogenesis of the murine eye. *Development* **127**, 945-956.

Danielian, P. S., Muccino, D., Rowitch, D. H., Michael, S. K. and McMahon, A. P. (1998). Modification of gene activity in mouse embryos in utero by a tamoxifen- inducible form of Cre recombinase. *Curr. Biol.* **8**, 1323-1326.

DasGupta, R. and Fuchs, E. (1999). Multiple roles for activated LEF/TCF transcription complexes during hair follicle development and differentiation. *Development* **126**, 4557-4568.

Dimanlig, P. V., Faber, S. C., Auerbach, W., Makarenkova, H. P. and Lang, R. A. (2001). The upstream ectoderm enhancer in Pax6 has an important role in lens induction. *Development* **128**, 4415-4424.

Eastman, Q. and Grosschedl, R. (1999). Regulation of LEF-1/TCF transcription factors by Wnt and other signals. *Curr. Opin. Cell Biol.* **11**, 233-240.

Faber, S. C., Dimanlig, P., Makarenkova, H. P., Shirke, S., Ko, K. and Lang, R. A. (2001). Fgf receptor signaling plays a role in lens induction. *Development* **128**, 4425-4438.

Furuta, Y. and Hogan, B. L. M. (1998). BMP4 is essential for lens induction in the mouse embryo. *Genes Dev.* **12**, 3764-3775.

Gotoh, N., Ito, M., Yamamoto, S., Yoshino, I., Song, N., Wang, Y., Lax, I., Schlessinger, J., Shibuya, M. and Lang, R. A. (2004). Tyrosine phosphorylation sites on FRS2alpha responsible for Shp2 recruitment are critical for induction of lens and retina. *Proc. Natl. Acad. Sci. USA* **101**, 17144-17149.

Grindley, J. C., Davidson, D. R. and Hill, R. E. (1995). The role of Pax-6 in eye and nasal development. *Development* **121**, 1433-1442.

Harada, N., Tamai, Y., Ishikawa, T., Sauer, B., Takaku, K., Oshima, M. and Taketo, M. M. (1999). Intestinal polyposis in mice with a dominant stable mutation of the beta-catenin gene. *EMBO J.* **18**, 5931-5942.

He, X., Semenov, M., Tamai, K. and Zeng, X. (2004). LDL receptor-related proteins 5 and 6 in Wnt/beta-catenin signaling: arrows point the way. *Development* **131**, 1663-1677.

Hill, R. E., Favor, J., Hogan, B. L., Ton, C. C., Saunders, G. F., Hanson, I. M., Prosser, J., Jordan, T., Hastie, N. D. and van Heyningen, V. (1991). Mouse small eye results from mutations in a paired-like homeobox- containing gene. *Nature* **354**, 522-525.

Hoffmans, R., Stadeli, R. and Basler, K. (2005). Pygopus and legless provide essential transcriptional coactivator functions to Armadillo/beta-Catenin. *Curr. Biol.* **15**, 1207-1211.

Joyner, A. L. I. (ed.) (1995). *Gene Targeting: A Practical Approach* (*The Practical Approach Series*). New York: IRL Press at Oxford University Press.

Kamachi, Y., Uchikawa, M., Tanouchi, A., Sekido, R. and Kondoh, H. (2001). Pax6 and SOX2 form a co-DNA-binding partner complex that regulates initiation of lens development. *Genes Dev.* **15**, 1272-1286.

Kaufman, M. H. (1992). *The Atlas of Mouse Development*. San Diego: Academic Press.

Kleinjan, D. A., Seawright, A., Schedl, A., Quinlan, R. A., Danes, S. and van Heyningen, V. (2001). Aniridia-associated translocations, DNase hypersensitivity, sequence comparison and transgenic analysis redefine the functional domain of PAX6. *Hum. Mol. Genet.* **10**, 2049-2059.

Kleinjan, D. A., Seawright, A., Elgar, G. and van Heyningen, V. (2002). Characterization of a novel gene adjacent to PAX6, revealing synteny conservation with functional significance. *Mamm. Genome* **13**, 102-107.

Kramps, T., Peter, O., Brunner, E., Nellen, D., Froesch, B., Chatterjee, S., Murone, M., Zullig, S. and Basler, K. (2002). Wnt/wingless signaling requires BCL9/legless-mediated recruitment of pygopus to the nuclear beta-catenin-TCF complex. *Cell* **109**, 47-60.

Lake, B. B. and Kao, K. R. (2003). Pygopus is required for embryonic brain patterning in Xenopus. *Dev. Biol.* **261**, 132-148.

Lang, R. A. (2004). Pathways regulating lens induction in the mouse. *Int. J. Dev. Biol.* **48**, 783-791.

Li, B., Mackay, D. R., Ma, J. and Dai, X. (2004). Cloning and developmental expression of mouse pygopus 2, a putative Wnt signaling component. *Genomics* **84**, 398-405.

Liu, H., Mohamed, O., Dufort, D. and Wallace, V. A. (2003). Characterization of Wnt signaling components and activation of the Wnt canonical pathway in the murine retina. *Dev. Dyn.* **227**, 323-334.

Macatee, T. L., Hammond, B. P., Arenkiel, B. R., Francis, L., Frank, D. U. and Moon, A. M. (2003). Ablation of specific expression domains reveals discrete functions of ectoderm- and endoderm-derived FGF8 during cardiovascular and pharyngeal development. *Development* **130**, 6361-6374.

Maretto, S., Cordenonsi, M., Dupont, S., Braghetta, P., Broccoli, V., Hassan, A. B., Volpin, D., Bressan, G. M. and Piccolo, S. (2003). Mapping Wnt/beta-catenin signaling during mouse development and in colorectal tumors. *Proc. Natl. Acad. Sci. USA* **100**, 3299-3304.

Medina-Martinez, O., Brownell, I., Amaya-Manzanares, F., Hu, Q., Behringer, R. R. and Jamrich, M. (2005). Severe defects in proliferation and differentiation of lens cells in Foxe3 null mice. *Mol. Cell. Biol.* **25**, 8854-8863.

Mosimann, C., Hausmann, G. and Basler, K. (2006). Parafibromin/Hyrax activates Wnt/Wg target gene transcription by direct association with beta-catenin/Armadillo. *Cell* **125**, 327-341.

Nakaya, M. A., Biris, K., Tsukiyama, T., Jaime, S., Rawls, J. A. and Yamaguchi, T. P. (2005). Wnt3alinks left-right determination with segmentation and anteroposterior axis elongation. *Development* **132**, 5425-5436.

Nottoli, T., Hagopian-Donaldson, S., Zhang, J., Perkins, A. and Williams, T. (1998). AP-2-null cells disrupt morphogenesis of the eye, face, and limbs in chimeric mice. *Proc. Natl. Acad. Sci. USA* **95**, 13714-13719.

Novak, A., Guo, C., Yang, W., Nagy, A. and Lobe, C. G. (2000). Z/EG, a double reporter mouse line that expresses enhanced green fluorescent protein upon Cre-mediated excision. *Genesis* **28**, 147-155.

Nusse, R. (2005). Wnt signaling in disease and in development. *Cell Res.* **15**, 28-32.

Parker, D. S., Jemison, J. and Cadigan, K. M. (2002). Pygopus, a nuclear PHD-finger protein required for Wingless signaling in Drosophila. *Development* **129**, 2565-2576.

Pinson, K. I., Brennan, J., Monkley, S., Avery, B. J. and Skarnes, W. C. (2000). An LDL-receptor-related protein mediates Wnt signalling in mice. *Nature* **407**, 535-538.

Popadiuk, C. M., Xiong, J., Wells, M. G., Andrews, P. G., Dankwa, K., Hirasawa, K., Lake, B. B. and Kao, K. R. (2006). Antisense suppression of pygopus2 results in growth arrest of epithelial ovarian cancer. *Clin. Cancer Res.* **12**, 2216-2223.

Robinson, J. M. and Vandre, D. D. (2001). Antigen retrieval in cells and tissues: enhancement with sodium dodecyl sulfate. *Histochem. Cell Biol.* **116**, 119-130.

Schwab, K., Patterson, L., Hartman, H., Song, N., Lang, R., Lin, X. and Potter, S. (2007). Pygo1 and Pygo2 roles in Wnt signaling in mammalian kidney development. *BMC Biol.* (in press).

Schwenk, F., Baron, U. and Rajewsky, K. (1995). A cre-transgenic mouse strain for the ubiquitous deletion of loxP-flanked gene segments including deletion in germ cells. *Nucleic Acids Res.* **23**, 5080-5081.

Smith, A. N., Miller, L. A., Song, N., Taketo, M. M. and Lang, R. A. (2005). The duality of beta-catenin function: a requirement in lens morphogenesis and signaling suppression of lens fate in periocular ectoderm. *Dev. Biol.* **285**, 477-489.
Spemann, H. (1901). Uber Correlationen in der Entwickelung des Auges. *Verh. Anat. Ges.* **15**, 61-79.
Stadeli, R. and Basler, K. (2005). Dissecting nuclear Wingless signalling: recruitment of the transcriptional co-activator Pygopus by a chain of adaptor proteins. *Mech. Dev.* **122**, 1171-1182.
Stump, R. J., Ang, S., Chen, Y., von Bahr, T., Lovicu, F. J., Pinson, K., de Iongh, R. U., Yamaguchi, T. P., Sassoon, D. A. and McAvoy, J. W. (2003). A role for Wnt/beta-catenin signaling in lens epithelial differentiation. *Dev. Biol.* **259**, 48-61.
Sullivan, C. H., Braunstein, L., Hazard-Leonards, R. M., Holen, A. L., Samaha, F., Stephens, L. and Grainger, R. M. (2004). A re-examination of lens induction in chicken embryos: in vitro studies of early tissue interactions. *Int. J. Dev. Biol.* **48**, 771-782.
Thompson, B. J. (2004). A complex of Armadillo, Legless, and Pygopus coactivates dTCF to activate wingless target genes. *Curr. Biol.* **14**, 458-466.
Thompson, B., Townsley, F., Rosin-Arbesfeld, R., Musisi, H. and Bienz, M. (2002). A new nuclear component of the Wnt signalling pathway. *Nat. Cell Biol.* **4**, 367-373.
Tolwinski, N. S. and Wieschaus, E. (2004). A nuclear escort for beta-catenin. *Nat. Cell Biol.* **6**, 579-580.
Townsley, F. M., Cliffe, A. and Bienz, M. (2004). Pygopus and Legless target Armadillo/beta-catenin to the nucleus to enable its transcriptional co-activator function. *Nat. Cell Biol.* **6**, 626-633.
Treisman, J. E. and Rubin, G. M. (1995). wingless inhibits morphogenetic furrow movement in the Drosophila eye disc. *Development* **121**, 3519-3527.
von Woellwarth, C. (1961). Die Rolle des Neuralleistenmaterials und der Temeratur bei der Determination der Augenlinse. *Embryologica Nagoya* **6**, 219-242.
Wawersik, S., Purcell, P., Rauchman, M., Dudley, A. T., Robertson, E. J. and Maas, R. (1999). BMP7 acts in murine lens placode development. *Dev. Biol.* **207**, 176-188.
Willert, K., Brown, J. D., Danenberg, E., Duncan, A. W., Weissman, I. L., Reya, T., Yates, J. R., 3rd and Nusse, R. (2003). Wnt proteins are lipid-modified and can act as stem cell growth factors. *Nature* **423**, 448-452.
Williams, S. C., Altmann, C. R., Chow, R. L., Hemmati-Brivanlou, A. and Lang, R. A. (1998). A highly conserved lens transcriptional control element from the Pax-6 gene. *Mech. Dev.* **73**, 225-229.
Zhang, J., Hagopian-Donaldson, S., Serbedzija, G., Elsemore, J., Plehn-Dujowich, D., McMahon, A. P., Flavell, R. A. and Williams, T. (1996). Neural tube, skeletal and body wall defects in mice lacking transcription factor AP-2. *Nature* **381**, 238-241.
Zhang, X., Friedman, A., Heaney, S., Purcell, P. and Maas, R. L. (2002). Meis homeoproteins directly regulate Pax6 during vertebrate lens morphogenesis. *Genes Dev.* **16**, 2097-2107.